

# Two dimensional time dependent simulation of the subcritical flow in a staggered tube bundle using a subgrid scale model

D. Bouris, G. Bergeles \*

National Technical University of Athens, Laboratory of Aerodynamics, Department of Mechanical Engineering, Heroon Polytechniou 5, 15700, Zografou, Athens, Greece

Received 20 April 1997; accepted 24 October 1998

## Abstract

Numerical calculation of subcritical flow in tube bundles is a difficult task since transitional effects as well as vortex shedding are important characteristics of the flow field. In the present paper a time dependent simulation using a subgrid scale model is performed in two dimensions for the subcritical flow through a staggered tube bundle. Previous time dependent simulations of the same flow using the  $k-\varepsilon$  turbulence model unfortunately lead to a steady state solution, which underpredicted turbulence quantities and recirculation lengths. Thus a novel approach is introduced, using a subgrid scale model for the calculation of the eddy viscosity. The methodology that is used strongly resembles a large eddy simulation even though it is performed in two dimensional space. A filtering procedure is used to remove the vortex shedding frequency from the velocity data thus allowing a calculation of the turbulence fluctuations. Calculated vortex shedding frequencies, periodic and turbulence velocity fluctuations and integral time scales are in good agreement with experimental measurements. © 1999 Elsevier Science Inc. All rights reserved.

**Keywords:** Time dependent simulation; Tube bundles; Subcritical flow; Subgrid scale model

## Notation

$C_s$	sub-grid scale constant	$U_0$	mean velocity of upstream flow entering the tube bundle ( $\text{m s}^{-1}$ )
$C_x, C_y$	longitudinal and transverse spacing of tube centers in tube bundle (m)	$w_0$	$= \tan(\pi f_0 dt)$ , function of vortex shedding frequency $f_0$
$d$	tube diameter (m)	$x, y$	Cartesian coordinate directions
$f$	frequency (Hz)	$Y$	normal distance from wall (m)
$H_{\text{Notch}}(f)$	Notch filter for the Fourier transform of a velocity time series.	$y^+$	$= Y\rho(\tau_w/\rho)^{1/2}\mu^{-1}$ , non-dimensional normal distance from wall
$k$	turbulence kinetic energy per unit mass ( $\text{m}^2 \text{s}^{-2}$ )	<i>Greek</i>	
$l_\xi, l_\eta$	metric coefficients related to orthogonal curvilinear coordinates	$\Delta$	filter width (m)
$R(\tau)$	autocorrelation function	$\Delta\xi, \Delta\eta$	grid increments in physical space in $\xi$ and $\eta$ directions, respectively (m)
$\text{Re}$	$= U_0 d \rho / \mu$ , Reynolds number	$\varepsilon$	rate of turbulence kinetic energy dissipation per unit mass ( $\text{m}^2 \text{s}^{-3}$ )
$S_{\xi\eta}$	total rate of strain ( $\text{s}^{-1}$ )	$\mu, \mu_t$	molecular and eddy viscosity, respectively ( $\text{kg m}^{-1} \text{s}^{-1}$ )
$ S $	$= (2S_{\xi\eta} S_{\xi\eta})^{1/2}$ , ( $\text{s}^{-1}$ )	$\mu_{\text{eff}}$	$= \mu_t + \mu$ , effective viscosity for sub-grid scale model ( $\text{kg m}^{-1} \text{s}^{-1}$ )
$\text{StH}$	$= fd/U_0$ , Strouhal number	$\xi, \eta$	orthogonal curvilinear coordinate directions
$T$	$= tU_0/d$ , non-dimensional time	$\rho$	fluid density ( $\text{kg m}^{-3}$ )
$t, \tau$	time (s)	$\sigma_{\xi\xi}, \sigma_{\eta\eta}, \sigma_{\xi\eta}$	normal and cross rate of strain components ( $\text{s}^{-1}$ )
$T_E$	Integral time scales (s)	$\tau_w$	shear stress at wall ( $\text{kg m}^{-1} \text{s}^{-2}$ )
$u'$ r.m.s.	root mean square of turbulent velocity fluctuation $u'$ ( $\text{m s}^{-1}$ )	$\tau_E$	Eulerian dissipation time scales or micro time scales (s)
$u, v$	velocities in $\xi$ and $\eta$ directions respectively ( $\text{m s}^{-1}$ )	$\omega$	frequency range around $w_0$ to filter out, expressed as a fraction of $w_0$

\* Corresponding author. E-mail: bergeles@fluid.mech.ntua.gr.

## 1. Introduction

The purpose of the present work is to use a time dependent simulation with a subgrid scale model to predict the subcritical flow through a staggered tube bundle. The flow field through tube bundles is of vital importance to heat exchanger operation and design but is difficult to calculate numerically, especially if the flow is in the subcritical regime where boundary layer transition occurs. Experimental studies of such flows have proven that there are unsteady phenomena such as vortex shedding and jet flapping (Hill et al., 1986; Balabani and Yianneskis, 1996) which are governed by different mechanisms depending on the tube row and the position within the tube bundle. Other factors which affect the periodicity of the flow are the Reynolds number, the arrangement and spacing of the tube bundle, tube surface roughness etc. In addition to the complexity arising from the flow instabilities in the tube bundle, one must also consider whether the flow is turbulent or laminar. Flows in heat exchanger tube bundles are usually subcritical (mixed, transition to turbulence occurs after separation) or critical (predominantly turbulent, only part of the boundary layer developing on the tube surface is laminar). In critical flows, transition to turbulence occurs before separation and turbulence is prominent in the rest of the boundary layer and in the flow inside the bundle (Zukauskas, 1989). The combination of the flow instabilities and the transitional phenomena present in the boundary layers makes this type of flow difficult to model numerically. Statistical turbulence models associated with the solution of the Reynolds averaged Navier–Stokes equations (i.e. the  $k$ – $\epsilon$  eddy viscosity turbulence model) have not been able to correctly predict transitional phenomena which, in the case of tube bundles are also combined with streamline curvature and turbulence anisotropy (Balabani et al., 1994; Bergeles et al., 1996). The result is an underprediction of the turbulence levels in the tube bundle. Furthermore, attempts to calculate the instabilities of the flow often fail due to the increased damping produced by eddy viscosity models. Braun and Kudriavtsev (1995) performed a numerical visualization of the laminar flow in a staggered tube bundle calculating instabilities and vortex shedding inside the tube bundle. However, apart from being a laminar flow calculation, a Cartesian grid was used and the curved surfaces of the tubes were approximated with a series of steps defined by the grid. Zdravistch et al. (1995) also performed calculations of the flow and heat transfer in staggered and in-line tube bundles by solving the Reynolds averaged Navier–Stokes equations. Their results showed good agreement when compared to experimental measurements but the Reynolds numbers that they studied corresponded to either laminar or fully turbulent flow so subcritical flow was not considered. Furthermore, their computations involved steady state solutions, neglecting effects of flow instabilities.

The numerical simulation presented here is a novel attempt to include the transitional and unsteady effects that appear in the subcritical flow through the first rows of a tube bundle arrangement. In statistical turbulence models associated with Reynolds averaging of the Navier–Stokes equations (e.g.  $k$ – $\epsilon$  turbulence model, Reynolds Stress Equation models etc.), assumptions are made which limit their validity for modeling the transitional, unsteady and streamline curvature characteristics of the type of flow studied here. On the other hand three dimensional large eddy simulation, which would be well suited for this kind of flow, has increased computer resource requirements and is often implemented using inadequate grid resolution or law of the wall boundary conditions.

In the present paper an attempt is made to combine the advantages of both approaches. Thus a two dimensional time dependent simulation is applied using a subgrid scale model

for modeling the eddy viscosity of the subgrid scales of turbulence. A fine grid resolution is used so that no-slip wall boundary conditions can be introduced thus overcoming the questionable validity of law of the wall boundary conditions. The goal is to simulate, through the Navier–Stokes equations, as many of the large scale characteristics of the flow as possible, associated with unsteadiness, transition and streamline curvature, while allowing smaller scale effects to be modeled by the subgrid scale model. The approach strongly resembles a large eddy simulation in two dimensions, a concept that has begun to appear in the literature lately (Hassan and Ibrahim, 1997; Barsamian and Hassan, 1997). It has been previously suggested that large eddy simulation should only be performed in three dimensions in order to capture the three dimensionality of turbulence (Rodi, 1993). However, inadequate resolution of the third spanwise direction is often observed. For quasi two dimensional flows a coarse resolution in the spanwise direction will almost certainly fail to simulate the three dimensional structures associated with turbulence (vortex stretching). In the case of transitional flows, although these structures exist, they are even less pronounced in the large scales as observed experimentally by Bergeles et al. (1996) for subcritical flow through a staggered tube bundle. For these particular types of flows, a two dimensional simulation is a point of interest. Furthermore, due to computer limitations, proper grid resolution near solid walls is often sacrificed in three dimensional simulations and law of the wall boundary conditions are implemented. In this sense, the simulation presented here is performed in two dimensions while attempting to resolve all of the turbulent boundary layer.

Recently, Balabani and Yianneskis (1996) performed experimental LDA measurements of the time resolved velocity field of a cross flow staggered tube bundle at subcritical Reynolds numbers. The measurements that were obtained involved dominant frequencies of the vortex shedding inside the tube bundle, mean velocity profiles and velocity fluctuation profiles as well as variables related to turbulence structure such as turbulence fluctuations and integral length scales. Here, a time dependent simulation of this flow is performed in two dimensions using a subgrid scale model on a collocated orthogonal curvilinear grid with direct resolution of the boundary layers in order to predict the transitional and unsteady phenomena that were experimentally observed. Steady state results arising from a simulation using the  $k$ – $\epsilon$  turbulence model are also presented. Filtering is performed in frequency space in order to compare predictions of turbulent velocity fluctuations and length scales with experimental measurements.

## 2. Numerical methodology

The Navier–Stokes equations are volume averaged according to Schumann (1975) with the control volumes being defined by the computational grid. In the present study the grid is orthogonal curvilinear and the equations are transformed accordingly (Batchelor, 1967). The volume average procedure is based on Green's theorem in space and so the final form of the equations closely resembles that of the Reynolds averaged equations when volume averaging is used. The equations are:

$$\frac{1}{l_\xi l_\eta} \frac{\partial}{\partial \xi} (\rho u l_\eta \Phi) + \frac{l}{l_\xi l_\eta} \frac{\partial}{\partial \eta} (\rho v l_\xi \Phi) - \frac{l}{l_\xi l_\eta} \frac{\partial}{\partial \xi} \left( \mu_{\text{eff}} \frac{l_\eta}{l_\xi} \frac{\partial \Phi}{\partial \xi} \right) - \frac{l}{l_\xi l_\eta} \frac{\partial}{\partial \eta} \left( \mu_{\text{eff}} \frac{l_\xi}{l_\eta} \frac{\partial \Phi}{\partial \eta} \right) = S_\Phi, \quad (1)$$

where  $(\Phi) = 1$  for the continuity equation,  $u$  for the momentum equation in the  $\xi$  direction and  $v$  for the momentum equation

in the  $\eta$  direction (for the contravariant directions on the grid see Fig. 1). The source terms on the right-hand side of Eq. (1) include the pressure gradient as well as other terms and are rather large but well known expressions in computational fluid dynamics. They are not presented here due to lack of space but they can be found in Antonopoulos (1979) or Mouzakis and Bergeles (1991). When volume averaging of the Navier–Stokes equations is performed, stress terms arise from the fluctuations (departure) from the volume averaged field, these fluctuations cannot be resolved by the grid and are modeled through a sub-grid scale model. The sub-grid scale stress model that is used here is that of Smagorinsky (1963) and Lilly (1967) and results in a turbulent viscosity  $\mu_t$  so that  $\mu_{\text{eff}} = \mu + \mu_t$ :

$$\mu_t = \rho(C_s \Delta)^2 |\bar{S}| = \rho(C_s \Delta)^2 (2\bar{S}_{\xi\eta}\bar{S}_{\xi\eta})^{1/2},$$

$$\bar{S}_{\xi\eta} = \frac{1}{2}(\sigma_{\xi\xi} + \sigma_{\eta\eta} + 2\sigma_{\xi\eta}),$$

$$\sigma_{\xi\xi} = 2\left(\frac{1}{l_\xi} \frac{\partial u}{\partial \xi} + \frac{v}{l_\xi l_\eta} \frac{\partial l_\xi}{\partial \eta}\right), \quad \sigma_{\eta\eta} = 2\left(\frac{1}{l_\eta} \frac{\partial v}{\partial \eta} + \frac{u}{l_\xi l_\eta} \frac{\partial l_\eta}{\partial \xi}\right), \quad (2)$$

$$\sigma_{\xi\eta} = \frac{1}{l_\xi} \frac{\partial v}{\partial \xi} + \frac{1}{l_\eta} \frac{\partial u}{\partial \eta} - \frac{v}{l_\xi l_\eta} \frac{\partial l_\eta}{\partial \xi} - \frac{u}{l_\xi l_\eta} \frac{\partial l_\xi}{\partial \eta},$$

where the  $C_s$  constant is taken here to be 0.1 (as in e.g. Breuer and Pourquie, 1996; Werner and Wengle, 1991. For a discussion on the value of this coefficient see Mason and Callen, 1986) and  $\Delta = (\Delta\xi\Delta\eta)^{1/2}$  as defined by the grid. Discretisation of the equations is applied using second order central differences except for the convection terms which are discretised using the Bounded Second Order Upwind (BSOU) scheme of Papadakis and Bergeles (1995). This upwind differencing scheme allows second order accuracy, thus overcoming the problems of numerical diffusion associated with first order upwind differencing, while being constantly bounded as opposed to some third order schemes (e.g. QUICK). It should be pointed out that the velocities are always defined as being parallel to the local grid lines while  $l_\xi$  and  $l_\eta$  are spatially varying metric coefficients related to the orthogonal curvilinear coordinates. They connect increments  $d\xi$  and  $d\eta$  of  $\xi$  and  $\eta$  in transformed space to increments of physical distance  $\Delta\xi$  and  $\Delta\eta$  as  $\Delta\xi = l_\xi d\xi$  and  $\Delta\eta = l_\eta d\eta$ . Discretisation in time is expressed through a first order, fully implicit Euler scheme. Although the scheme is of first order accuracy, the fact that it is fully implicit allows stability even for large time steps.

Solution of the equations is based on the SIMPLE algorithm for pressure correction (Patankar and Spalding, 1972) except that in the present approach the variables are collocated

on the grid so the Rhie and Chow (1983) interpolations are used in the pressure equation for the velocities on the volume cell faces.

No-slip boundary conditions are imposed at the walls instead of using law of the wall approximations. Such approximations have been successfully used in the past (Schumann, 1975; Werner and Wengle, 1991) but in the present situation, the curved cylinder walls and the relatively low Reynolds number do not comply with the assumptions on which law of the wall approximations are based. The use of no-slip boundary conditions requires a very fine grid near the wall and this will be evaluated during the computations. For the present situation of turbulent flow through a tube bundle it was assumed that the upstream flow was laminar so no fluctuations were introduced at the inlet. At the outlet, zero gradients were assumed in the streamwise direction.

### 3. Calculation of subcritical flow through a tube bundle

The staggered tube bundle under study has a relative spacing of  $C_x/d = 1.6$ ,  $C_y/d = 3.6$  ( $d = 10$  mm) and the Reynolds number of the flow is  $Re = U_0 \rho d / \mu = 9300$  which corresponds to a mixed (subcritical) flow with transition of the boundary layer from laminar to turbulent near separation. The flow through a tube bundle has been previously calculated using the Reynolds averaged approach with the  $k-\epsilon$  turbulence model in Balabani et al. (1994). It was observed that the predictions of the mean velocity were in generally good agreement with experimental measurements but the turbulence intensities were underpredicted. Attempts were made to improve the predictions through the use of modifications to the  $k-\epsilon$  turbulence model for streamline curvature (Balabani et al., 1994) as well as with the use of Low Reynolds models for the walls (Bergeles et al., 1996) with no significant improvement. It was concluded that the simulation of transitional effects in the development of the boundary layer as well as possible unsteadiness of the flow was outside the capabilities of this type of approach. Attempts to model the time dependent nature of the flow with the  $k-\epsilon$  turbulence model lead to a steady state solution due to the damping introduced by the  $k-\epsilon$  eddy viscosity. Rodi (1993) used the  $k-\epsilon$  model, with wall functions as well as with a two zone modeling approach for the boundary layer, in a simulation of the turbulent flow past a square rod. He also found excessive damping occurring with the use of the  $k-\epsilon$  model while even the use of a Reynolds Stress Equation turbulence

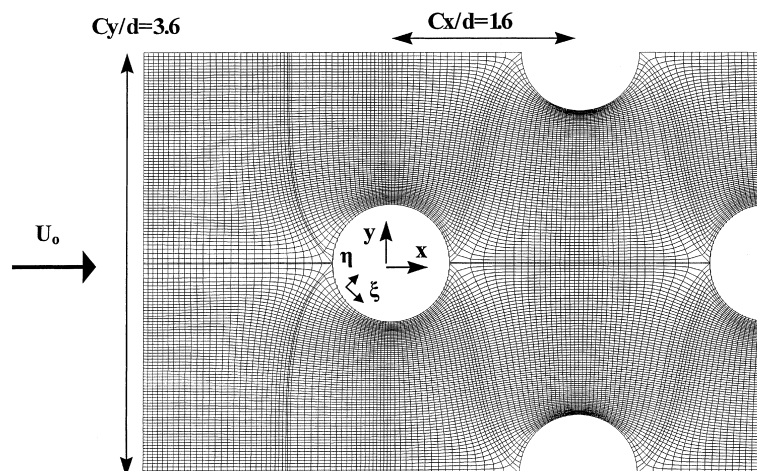


Fig. 1. Close-up of orthogonal curvilinear grid (280 × 280) used in the time dependent simulation of turbulent flow through a staggered tube bundle.

model showed irregular behavior since the periodic and turbulent frequencies could not be simultaneously predicted. The case of the square rod is different from that of a circular cylinder since the separation point is always fixed at the leading edge of the rod while for a circular cylinder the separation point is more difficult to predict numerically. In light of these experiences, the present time dependent simulation using a subgrid scale model was used. This allows the direct calculation of boundary layer transition as well as effects of large scale turbulence anisotropy and streamline curvature. Other characteristics of the flow field are the periodic vortex shedding mechanisms and jet flapping as were observed from the experimental measurements of Balabani and Yianneskis (1996).

The simulation is performed in orthogonal curvilinear coordinates and a close up of the computational grid that was used ( $280 \times 280$ ) is shown in Fig. 1. This is the area around the center tube of the first vertical row of tubes (Fig. 2) and the center of this tube represents the origin of the  $x$ - $y$  Cartesian frame of reference to be used hereafter in the presentation of results. The grid covers the whole experimental set up used in Balabani and Yianneskis (1996) so there is no uncertainty regarding boundary conditions at the side walls. Half cylinders on the solid walls of the experimental configuration are included in the simulation. As previously stated, the inlet conditions are those of a laminar uniform velocity profile with  $U_0 = 0.93 \text{ m s}^{-1}$ . This approximation is considered valid since the flow instabilities arising inside the tube bundle are mostly due to phenomena present at separation while the fluctuations of the flow velocity at the inlet position were measured at 8% of the mean velocity. No-slip boundary conditions were used at all solid wall boundaries and the values of  $y^+ = Y\rho(\tau_w/\rho)^{0.5}/\mu$  during calculations were found to vary between 0.16 and 27 with the maximum value arising at the stagnation point of the second cylinder in the third row (third row cylinder in Fig. 1). This value of  $y^+$  is too large for a simulation of the sublayer but the orthogonality condition of the curvilinear grid makes it difficult to create grid cells that come closer to the wall in these areas. Fortunately the problem is limited to the two cells in that immediate region and all other values of  $y^+$  were perfectly acceptable. Calculations of the same configuration using general coordinate system calculations with finer grid resolutions (Karadimos, 1995) showed that the region near the separation point is much more influential to the results than the stagnation regions where mesh distortion problems usually arise. The adequacy of the grid regarding effects of numerical diffusion due to spatial discretisation was also investigated. Steady state simulations using first and second order discretisation schemes

on the same configuration (Bouris, 1997) showed that increasing the spatial discretisation twofold (twice as many grid points in both directions) had minimal effect on the results. This can also be attributed to the fact that the Reynolds number corresponds to a transitional and not a fully turbulent flow. It is possible however that in the unsteady simulation the smallest resolved scales, e.g.  $L < 4\lambda$  might be affected by numerical diffusion especially in relation to the smaller turbulent viscosity calculated by the subgrid scale model in relation to the  $k$ - $\epsilon$  model. These effects are expected to be limited but should be considered when assessing the results. The initial field from which calculations were started was obtained from the steady state  $k$ - $\epsilon$  calculation allowing periodicity to be attained faster than from an initially zero velocity field. Numerical computations were performed on an IBM PowerPC with a PowerPC604 processor at 140 SPECfp. For the smallest time step used, about 100–140 iterations were needed for the maximum equation residual to be less than 0.1% at each time step and this consumed 12 min of CPU time.

In Fig. 2 the iso-vorticity regions in the tube bundle are presented. It can be discerned that flow perturbations due to the unsteady nature of the vortex shedding become more prominent for the downstream rows of the tube bundle. This was the reason that steady state calculations were originally considered. However, even the more restrained perturbation present after the first row will definitely affect the area in which measurements were performed (top half of Fig. 1) and fully justifies the unsteady calculation (instead of the steady state). Measurements were performed at sampling rates of 1–4 kHz and blocks of 6000 data points were recorded; the computational time steps were chosen accordingly. The first time step used was  $dt = 0.001 \text{ s}$  and the time series of the velocity component in the main flow direction at  $x/d = 1.6$ ,  $y/d = 0.6$  is presented in Fig. 3. Fourier transform of the time series (Fig. 4) gives a dominant frequency of  $f = 35 \text{ Hz}$  or a Strouhal number of  $\text{St}_h = fd/U_0 = 0.376$  in good agreement with the experimentally measured values of  $f = 34 \text{ Hz}$ ,  $\text{St}_h = fd/U_0 = 0.366$  (Balabani and Yianneskis, 1996). In Fig. 3 the periodic and turbulent components of the instantaneous velocity are also shown. These are calculated by applying a notch filter (Press et al., 1987) to the Fourier transform (Fig. 4) of the velocity time series

$$H_{\text{Notch}}(f) = \frac{w^2 - w_0^2}{(w - i\omega w_0)^2 - w_0^2}, \quad w = \tan(\pi f dt), \quad (3)$$

where  $w_0$  represents the dominant (vortex shedding) frequency and  $\omega$  is the width of the frequency range around it (here

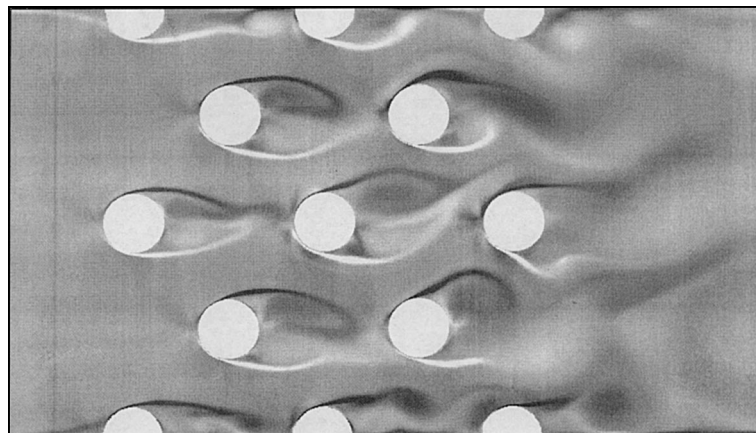


Fig. 2. Iso-vorticity regions of turbulent flow through a staggered tube bundle.

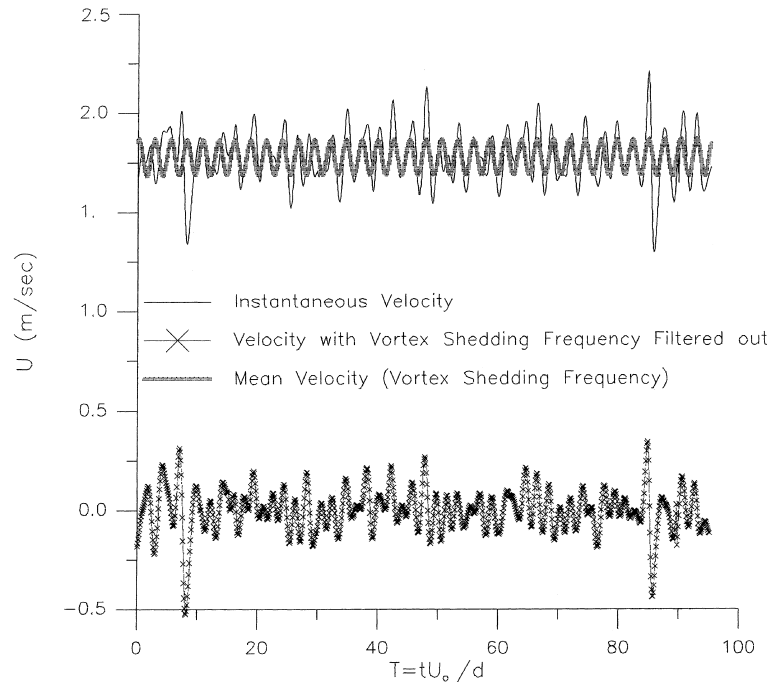


Fig. 3. Time series of instantaneous velocity component in the  $x$  direction and periodic and turbulent velocity fluctuations at  $x/d=1.6$ ,  $y/d=0.6$ .

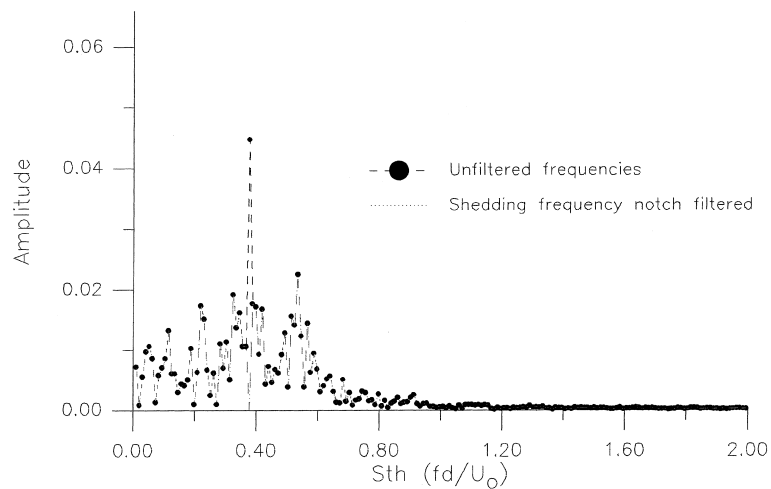


Fig. 4. Non-dimensional frequency spectrum (Strouhal number) of instantaneous velocity component in the  $x$  direction at  $x/d=1.6$ ,  $y/d=0.6$ .

$\omega = 0.1$  was used), expressed as a fraction of  $w_0$ , which must be removed from the spectrum. The resulting frequency spectrum should be that of all fluctuations other than those corresponding to the vortex shedding frequency and can be attributed to turbulence. An inverse Fourier transform gives the turbulent velocity fluctuations and subtracting these from the instantaneous velocity gives the periodic velocity time series.

A smaller time step was also used for calculation of the flow field. The time step was  $dt = 0.00025$  s while the largest sampling frequency used in the experimental measurements was 4 kHz. Balabani and Yianneskis (1996) measured Eulerian dissipation time scales or micro time scales ( $\tau_E$ ) which were found to have a mean value of 0.7 ms across the flow field. According to the Nyquist criterion, in order to calculate a frequency  $fc$  one must use a sampling rate of  $h = 1/2fc$  so for the micro time scales' frequency (1/0.7 kHz) the sampling rate or time step must be  $dt = 0.35$  ms. Since this is only for the mean value of  $\tau_E$

the choice of a smaller time step (as here  $dt = 0.25$  ms) might be superfluous in certain points of the flow. Also, the numerical grid will most probably not be fine enough to simulate the length scales which correspond to the micro time scales and so the SGS model will play an important role in the simulation for certain points of the flow. Nonetheless, it is interesting to see the effect of the time step on the results of the simulation. Through a Fourier transform, the dominant frequency for  $dt = 0.25$  ms is found to give a Strouhal number of  $Sth = fd/U_0 = 0.357$  in good agreement with the experimental value of 0.366 and only 5% smaller than the value from the first time step (0.376).

The calculated mean velocity distribution as well as the turbulent and periodic fluctuations will now be presented and compared with the results obtained from the  $k-\epsilon$  turbulence model (Balabani et al., 1994) and with experimental measurements (Balabani and Yianneskis, 1996). The velocity time

series for which integration was performed was  $\sim 100T$  ( $T = tU_0/d$ ) for  $dt = 1$  ms which corresponds to  $\sim 37$  shedding periods (taking  $St_h = 0.376$ ). For  $dt = 0.25$  ms, time integration has been performed for  $T \sim 120$  corresponding to about 46 shedding periods and  $\sim 5000$  time steps (experimental measurements used 6000 data points).

In Fig. 5 the mean velocity profiles (from time averaging of the whole time series in accordance with the experimentally provided values, Balabani and Yianneskis, 1996) are presented for  $dt = 0.1$  ms and the agreement with experimental measurements is acceptable but discrepancies are evident in the recirculation zones. It should be mentioned that the two sets of experimental data shown in Fig. 5 are the results obtained at two different runs for exactly the same operating conditions and apparatus. In a personal communication (Balabani, 1996) regarding the time resolved measurements (Balabani and Yianneskis, 1996) this was attributed to the positioning error of the LDA equipment. Another reason for the discrepancies between numerical and experimental results is the relatively small integration time (although covering 30 shedding periods it is actually  $\sim 1000$  time steps) which might affect the results

especially in the recirculation regions where unsteady phenomena are more prominent. A larger integration time was used with the smaller time step and the resulting mean velocity profiles are presented in Fig. 6. The mean velocity profiles seem to be in better agreement near the recirculation regions when compared to the previous time step. Generally though, the overall differences resulting from the change in time step are small and limited to these regions. The authors do not believe that the differences are due to the first order time discretisation scheme since in the other areas of the flow the mean velocity computations seem to be independent of the time step as does the Strouhal number. The maximum local Courant number in the calculations was about 10, which is acceptable for an implicit scheme. The differences in the recirculation zones might be due to the larger time integration used for the results of the smaller time step. The number of time steps used in the time integration is rather small when compared to large eddy simulations but one should keep in mind that the number of shedding periods over which integration is performed is perfectly adequate (Breuer and Pourquie, 1996, used about  $10^5$  time steps but covered only 13

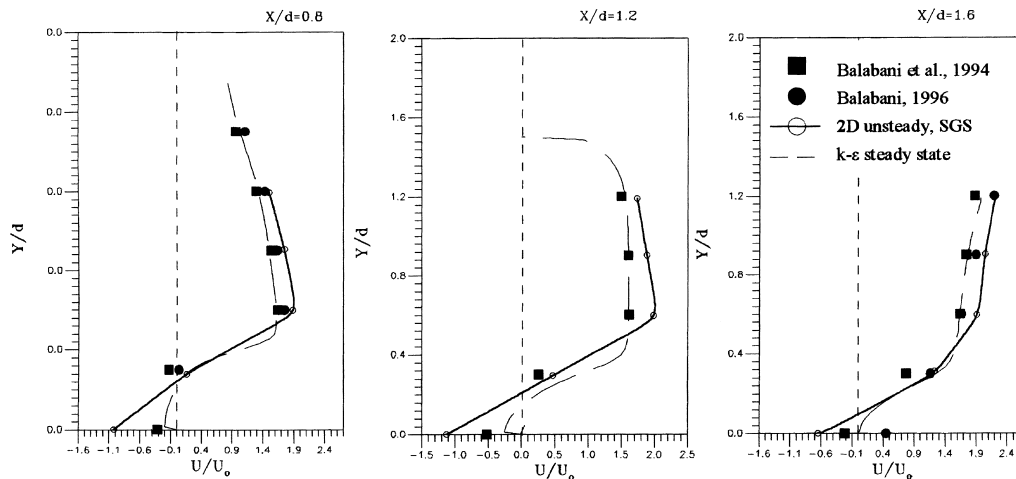


Fig. 5. Mean velocity component in the  $x$  direction as predicted from time dependent simulation with SGS model and from Reynolds averaged approach using the  $k-\epsilon$  turbulence model. Comparison with experimental measurements.

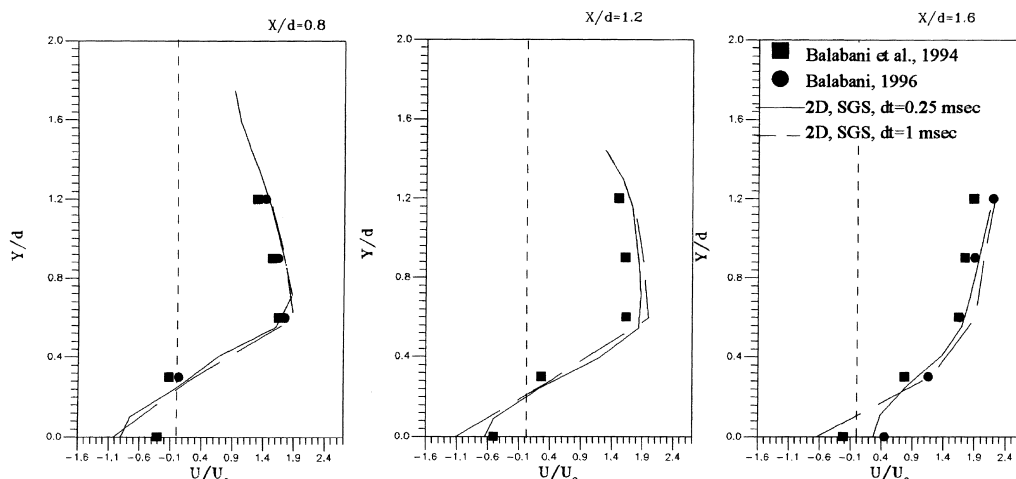


Fig. 6. Mean velocity component in the  $x$  direction as predicted from time dependent simulation with SGS model using two different time steps and comparison with experimental measurements.

shedding periods for the fully turbulent flow past a square rod). Furthermore, the time step has been chosen to be comparable to the sampling frequency of the experimental measurements. This is important since, for smaller time steps, higher frequencies would be resolved that have not been measured experimentally and a comparison of the results would not be indicative. Also, a smaller time step would correspond to turbulent scales that would have to be represented by the Smagorinsky SGS model. A better evaluation of the effect of the SGS model might have been warranted but in previous studies more advanced SGS models did not bring significant improvements (Breuer and Pourquie, 1996; Hartel and Kleiser, 1992).

In Fig. 7 the velocity fluctuations including the periodic motion are compared to the experimental measurements which were obtained without filtering of the frequency spectrum. Results shown are with the  $dt=1$  ms time step which is the sampling frequency at which most measurements were performed. The current predictions are in better agreement with the measurements than the  $k-\varepsilon$  model predictions. Not only are the fluctuation levels closer to the experimental measurements, but the trends of the profiles are also in better agreement. This indicates that the present simulation of the development and separation of the boundary layer on the front of the first cylinder correctly predicts the production of turbulence and any transitional phenomena that may appear in the boundary layer or the shear layer after separation.

Filtering of the measured velocity fluctuations was performed by Balabani and Yianneskis (1996) in order to remove the dominant vortex shedding frequency. The filtering procedure that they used is the same as the one used here i.e. notch filtering. Comparison of the filtered fluctuating velocity distributions, which represent fluctuations due to turbulence, is presented in Fig. 8. At most positions, the computations are in satisfactory agreement with the measurements but there are some points where the non-periodic fluctuation level remains high when compared to the experiments and the  $k-\varepsilon$  computation. This could indicate that the predicted level of fluctuations due to periodic movement is underestimated by the numerical procedure since its removal has only a small effect on the distribution. On the other hand, one should keep in mind that the frequency spectrum resulting from numerical calculations is much more discrete than that of the experimental measurements. Therefore, removing a notch of fre-

quencies around  $f_0$  will remove less energy than in the case of the experimental spectrum. Furthermore, it can be seen from Fig. 4 that there is a lot of energy in the low frequency region around  $f_0$  but almost no energy in the higher frequency region where the inertial sublayer should be. The higher frequencies, which correspond to small length scales, are modeled by the SGS model and do not appear in the frequency spectrum while any three dimensional effects tend to be amplified as larger scales in two dimensions (Tamura et al., 1990) resulting in extra low frequency fluctuations. All of the above might be an explanation for the excess kinetic energy attributed to non-periodic motion at certain positions, as seen in Fig. 8. In any case, the results are much closer to physical reality than those of previous attempts using the  $k-\varepsilon$  model, which failed to predict any periodic motion and thus underestimated the total velocity fluctuation (Fig. 7).

The autocorrelation function  $R(\tau)$  is defined as

$$R(\tau) = \frac{\overline{u'(\vec{x}, t)u'(\vec{x}, t + \tau)}}{\overline{u'(\vec{x}, t)^2}}, \quad (4)$$

where the velocities are the turbulent fluctuations as calculated from the filtering procedure. The integral time scales  $T_E$  can be calculated

$$T_E = \int_0^{\infty} R(\tau) d\tau. \quad (5)$$

In practice, the integral in Eq. (5) is usually calculated from  $\tau=0$  to the first point at which  $R(\tau)$  becomes zero. This is the way it was calculated from experimental measurements (Balabani and Yianneskis, 1996) and the comparison of predictions to measurements is presented in Fig. 9. When using the  $k-\varepsilon$  turbulence model, the integral time scales cannot be calculated from the autocorrelation function since such information is not available. They are usually calculated as  $T_E = 0.09(k^{3/2}/\varepsilon)/(2k/3)^{1/2}$  being highly dependent on all assumptions related to the  $k$  and  $\varepsilon$  equations and leading to rather large discrepancies between numerical predictions and experimental measurements. This has been applied here to the results obtained from the steady state  $k-\varepsilon$  model calculation (Balabani et al., 1994; Bergeles et al., 1996) and is also plotted in Fig. 9. Considering the above, the current predictions of the integral length scales presented in Fig. 9 are in good agreement

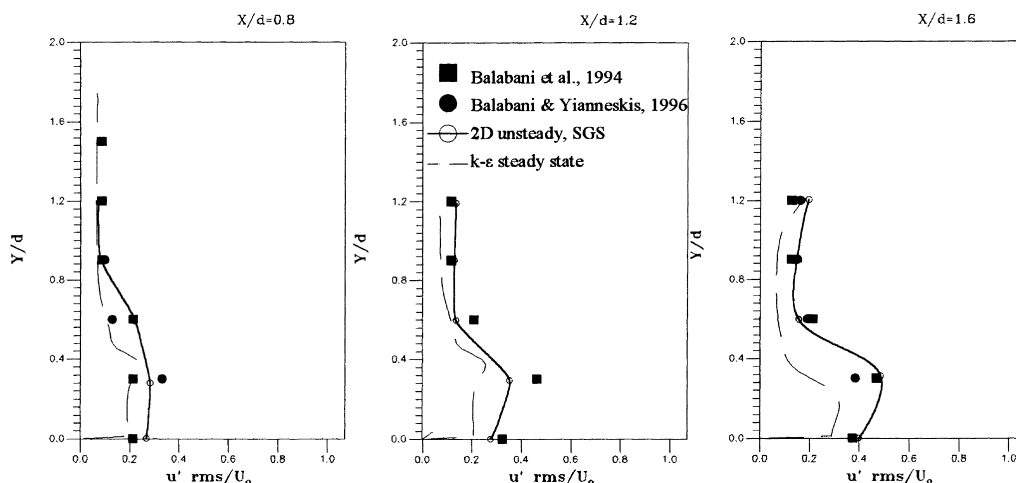


Fig. 7. Fluctuations (periodic + turbulent) of the velocity component in the  $x$  direction as predicted from time dependent simulation with SGS model and from Reynolds averaged approach using the  $k-\varepsilon$  turbulence model. Comparison with experimental measurements.

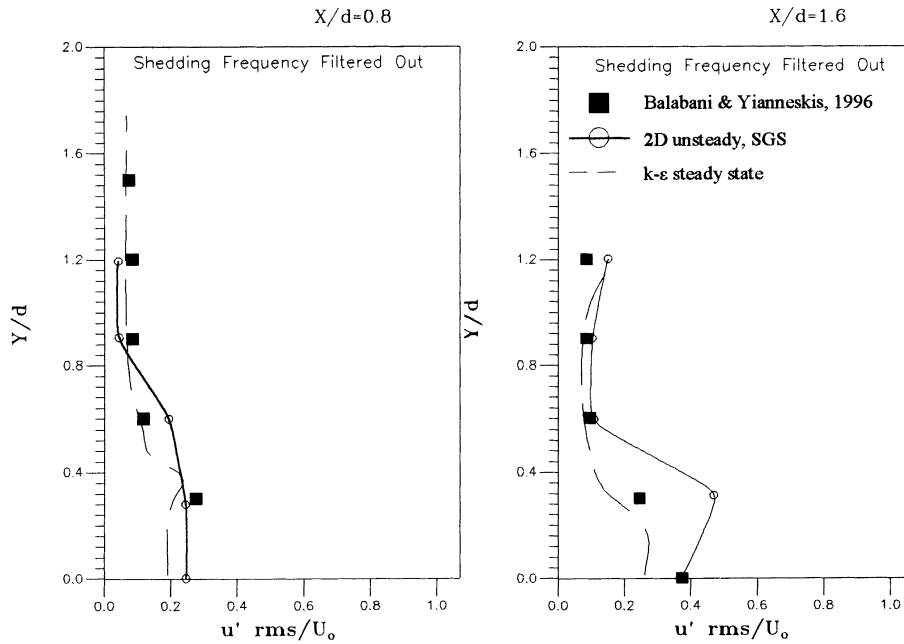


Fig. 8. Turbulent fluctuations of the velocity component in the  $x$  direction as predicted from time dependent simulation with SGS model and from Reynolds averaged approach using the  $k-\epsilon$  turbulence model. Comparison with experimental measurements. (Calculated from frequency filtering for the shedding frequency.)

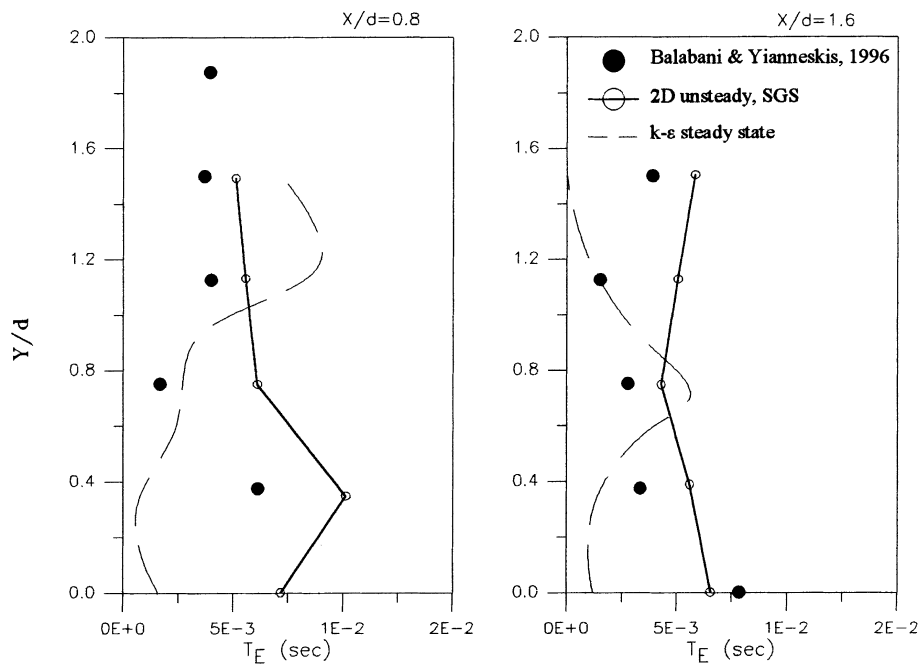


Fig. 9. Prediction of integral time scale distribution at two positions inside the staggered tube bundle. (Calculated from turbulent fluctuations only.) Comparison with experimental measurements and  $k-\epsilon$  model results.

with the measurements while it is evident that the  $k-\epsilon$  model calculations hardly follow the trend of the measured length scale distributions.

#### 4. Conclusions

The subcritical flow through a staggered tube bundle involves transitional effects which are coupled with the unsteady

nature of the flow and is a challenging numerical calculation. The two dimensional time dependent simulation using a subgrid scale model that was performed here is a novel attempt to include both of these physical mechanisms in a numerical calculation. In the present study, time dependent calculations of the subcritical cross flow through a staggered tube bundle have been performed in two dimensions with a subgrid scale model on a collocated orthogonal curvilinear grid. The whole experimental set-up has been resolved by the grid and com-



parison with experimental measurements has shown good agreement. The predicted vortex shedding frequency is found to be in very good agreement with the experimentally measured value and mean velocity profiles show acceptable agreement with slight discrepancies in the recirculation zones. The prediction of the velocity fluctuations is highly improved in relation to previous attempts using the  $k-\epsilon$  turbulence model. The unsteady phenomena as well as the direct simulation of the boundary layer and any transitional effects that may be present prove to be important when calculating such flows. The two dimensional calculation permitted a direct simulation of the boundary layers since if three dimensions were simulated the computational requirements would be overwhelming. Filtering of the velocity field so that the vortex shedding frequency is removed allows the comparison of the turbulent fluctuations and the integral length scales. The turbulent fluctuations seem to be slightly overpredicted but this could be due to the filtering of the discrete frequency spectrum which does not remove all of the periodic motion and results in some aliasing towards the turbulent fluctuations. The prediction of the integral length scales is in rather good agreement with the experimental measurements especially if one considers the fact that statistical turbulence models fail to predict such quantities related to the finer turbulent structures.

The use of a subgrid scale model in a two dimensional time dependent simulation shows interesting results for such flows where turbulence anisotropy, transitional effects and flow field periodicity are important aspects that are difficult to simulate. The purpose of the paper is not to suggest using the time dependent approach with subgrid scale modeling in place of traditional turbulence modeling approaches. Indeed, there are many points for discussion and the calculations presented here are intended only as a computational experiment in the use of subgrid scale models in two dimensional calculations of subcritical quasi-two dimensional flows.

The discrepancies that are observed should be considered under the following arguments. First of all the two dimensional simulation allows a better resolution of the boundary layer with no slip boundary conditions on the walls but it does not allow the effects of three dimensional phenomena to be included in the results. Although these are expected to be limited due to the quasi-two dimensional character of the flow field, the importance of the third dimension in turbulence simulation and especially transitional phenomena should not be overlooked. A simulation with a denser grid and a smaller time step might be warranted and the role of the SGS model in the simulation should be evaluated. This has been considered before in the literature and has not proven to be important, however when transitional phenomena are present the isotropy assumption associated with the Smagorinsky model does not have a firm physical basis. In assessing the reliability of the two dimensional time dependent simulation and the importance of a fine grid resolution in relation to a three dimensional large eddy simulation with a coarser grid, it should be pointed out that the conclusions are strongly related to the fact that the simulated flow is subcritical-transitional. In a fully turbulent flow the three dimensional effects might be more influential to the simulation.

## References

Antonopoulos, K., 1979. Prediction of flow and heat transfer in rod bundles. Ph.D. Thesis, Mechanical Engineering Department, Imperial College, London, UK.

Balabani, S., 1996. Personal communication regarding Balabani and Yianneskis.

Balabani, S., Yianneskis, M., 1996. An experimental study of the mean flow and turbulence structure of cross-flow over tube bundles. *Proc. Instn. Mech. Engrs.* 210, pp. 317–331.

Balabani, S., Bergeles, G., Burry, D., Yianneskis, M., 1994. Velocity characteristics of the crossflow over tube bundles. *Proceedings of the 7th International Symposium on Applications of Laser Anemometry to Fluid Mechanics*, Lisbon, 1994, vol. II, 39.3.1–39.3.8.

Barsamian, H., Hassan, Y., 1997. Large eddy simulation of turbulent crossflow in tube bundles. *Nuclear Engineering and Design* 172, 102–122.

Batchelor, G.K., 1967. *An Introduction to Fluid Dynamics*. Cambridge University Press.

Bergeles, G., Bouris-Burry, D., Yianneskis, M., Balabani, S., Kravaritis, A., Itskos, S., 1996. Effects of fouling on the efficiency of heat exchangers in lignite utility boilers. Final report, Joule II programme, Contract No. JOU2-CT92-0014.

Bouris, D., 1997. Numerical Investigation of the Flow Field and Fouling in Heat Exchangers, Ph.D. Thesis, Department of Mechanical Engineering, National University of Athens.

Braun, M., Kudriavtsev, V., 1995. Fluid flow structures in staggered banks of cylinders located in a channel. *J. Fluids Engineering* 117, 36–44.

Breuer, M., Pourquie, M., 1996. First experiences with LES of flows past bluff bodies. In: Rodi, W., Bergeles, G. (Eds.), *Proceedings of the 3rd International Symposium on Engineering Turbulence Modeling and Measurements*, Heraklion, Crete, Greece, 27–29 May. Elsevier, Amsterdam, pp. 177–186.

Hartel, C., Kleiser, L., 1992. Comparative Testing of Subgrid Scale Models for Wall Bounded Turbulent Flows. In: Hirsch Ch. et al. (Eds.), *Computational Fluid Dynamics* 92, vol. 1, Elsevier, pp. 215–222.

Hassan, Y., Ibrahim, W., 1997. Turbulence prediction in two-dimensional bundle flows using large eddy simulation. *Nuclear Technology* 119, 11–28.

Hill, R., Shim, K., Lewis, R., 1986. Sources of excitation in tube banks due to vortex shedding. *Proc. Instn. Mech. Engrs.* 200, No. C4, 293–301.

Karadimos, A., 1995. Calculations of turbulent flow in heat exchanger tube bundles with low Reynolds turbulence models, Diploma Thesis, Fluids Section, Department of Mechanical Engineering, National Technical University of Athens, Athens, Greece.

Lilly, D., 1967. The representation of small scale turbulence in numerical simulation experiments. In: Goldstine, H.H. (Ed.), *Proc. IBM Scientific Computing Symposium on Environmental Sciences*, IBM Form No. 320–1951, pp. 195–210.

Mason, P., Callen, N., 1986. On the magnitude of the subgrid scale eddy coefficient in large eddy simulations of turbulent channel flow. *J. Fluid Mechanics* 162, 439–462.

Mouzakis, F., Bergeles, G., 1991. Numerical prediction of turbulent flow over a two dimensional ridge. *Int. J. Num. Methods in Fluids* 12, 287–296.

Papadakis, G., Bergeles, G., 1995. A locally modified second order upwind scheme for convection terms discretisation. *Int. J. Num. Meth. Heat Fluid Flow* 5, 49–62.

Patankar, S.V., Spalding, D.B., 1972. A calculation procedure for heat, mass and momentum transfer in three dimensional parabolic flows. *Int. J. Heat and Mass Transfer* 15 (10), 1787.

Press, W., Flannery, B., Teukolsky, S., Vetterling, W., 1987. *Numerical Recipes*. Cambridge University Press.

Rhie, M.C., Chow, L.W., 1983. A numerical study of the turbulent flow past an air foil with trailing edge separation, *AIAA Journal* 21, 1525–1532.

Rodi, W., 1993. On the simulation of turbulent flow past bluff bodies. *J. Wind Eng. Ind. Aer.* 46 and 47, 3–19.

Schumann, U., 1975. Subgrid scale model for finite difference simulations of turbulent flows in plane channels and annuli. *J. Computational Physics* 18, 376–404.

- Smagorinsky, J., 1963. Monthly Weather Review 91, 99–164.
- Tamura, T., Ohta, I., Kuwahara, K., 1990. On the reliability of two-Dimensional simulation for unsteady flows around a cylinder-type structure. *J. Wind Engineering and Industrial Aerodynamics* 35, 275–298.
- Werner, H., Wengle, H., 1991. Large eddy simulation of turbulent flow over and around a cube in a plate channel. Proceedings of the 8th Symposium on Turbulent Shear Flows, 9–11 September, Techn. Univ. Munich. Springer, pp. 155–168.
- Zukauskas, A., 1989. High Performance Single Phase Heat Exchangers. Karni, J. (Ed.), Hemisphere Publishing Corporation, Ch. 12 and 13, pp. 241–289.
- Zdravistch, F., Fletcher, C., Behnia, M., 1995. Numerical laminar and turbulent fluid-flow and heat transfer predictions in tube banks. *Int. J. Num. Methods for Heat and Fluid Flow* 5 (8), 717–733.